

Detection of Contamination Defect on Ice Cream Bar Based on Fuzzy Rule and Absolute Neighborhood

LI Shaoli, YUAN Weiqi

(Computer Vision Group, Shenyang University of Technology, Shenyang 110870)

Abstract: The contamination proposed in this paper is a defect on the surface of ice cream bar, which is a serious security threat. So it is essential to detect this defect before launched on the market. A detection method of contamination defect on the ice cream bar surface is proposed, which is based on fuzzy rule and absolute neighborhood feature. Firstly, the ice cream bar surface is divided into several sub-regions via the defined adjacent gray level clustering method. Then the alternative contamination regions are extracted from the sub-regions via the defined fuzzy rule. At last, the real contamination regions are recognized via the relationship between absolute neighborhood gray feature and default threshold. The algorithm was tested in the self-built image database SUT-D. The results show that the accuracy of the method proposed in this paper is 97.32 percent, which increases 2.68 percent at least comparing to the other typical algorithms. It indicates that the superiority proposed in this paper, which is of actual use value.

Key words: Fuzzy Rule; Absolute Neighborhood; Icecream Bar; Contamination; Adjacent Gray Level Clustering

1 Introduction

Ice cream bar is the handle of popsicle, which could generate various defects in the process of the production, the manufacturers should execute strict quality assurance to ensure its hygiene^[1]. At present, the main detection methods for ice cream bar defects are manual measurement, which are luminous flux method and machine vision method. The manual measurement methods mainly rely on visual inspection through experienced artisans, which are inefficient to meet the requirements of modern automatic production line. Meanwhile, the manual operation may bring in new health hazard, such as hair, fingernail chipping and so on^[2]. The luminous flux method is usually used for detecting the contour deformable defects of ice cream bar, such as bowing and lateral bending, but is not effective to detect the defects on surface^[3-5]. The basic principle of machine vision method is acquiring the image of ice cream bar surface via imaging sensor and then detecting the defect using digital picture processing technique. This method could complete the whole defects

detection of ice cream bar surface, and possesses the advantages of high precision, high efficiency and repeatability. It is applied to surface defects detection of various workpieces, and is the mainstream method of ice cream bar detection at present^[6-8].

The contamination is a kind of defect on ice cream bar surface, which would affect hygiene safety seriously. Through literature retrieving, the researches of ice cream bar surface defects detection based on machine vision focus on crevice, mineral lineation and knot^[9-13]. The researches on contamination are few, described as follows. In 2015, CHEN proposed the contamination segment method based on adaptive local threshold. Its basic principle is acquiring the gray difference of original image and the image after average filtering, then the difference position is determined as the contamination defect region. The detection performance of this method relies on the size of filtering window and stated gray difference threshold, so it could not overcome the indeterminacy of defect size. SONG proposed the method of gradation histogram^[15]. Its basic principle is computing the smoothness of wood in certain re-

gion and estimating this region through the relationship between smoothness value and stated threshold value. However, the smoothness value in this method is affected by the region position, area and global illumination distribution of image, thus, it lacks robustness and cannot detect the defect properly. YUAN proposed a contamination detection method based on Union-Find and constraint set^[16]. In this method, the region of ice cream bar is clustered on gray via Union-Find, then the contamination region is detected through the defined 4 constraint rules. The 4 constraint rules are corresponding to 4 features, and the defect is detected via the relationship between feature value and threshold. It obtains a certain effect, but the wooden texture and dim spot are mistakenly identified, some contamination regions are also missed. Therefore, this method needs further improvement.

Aiming at the problem of contamination detection on ice cream bar surface, this paper puts forward an algorithm scheme based on fuzzy rule and absolute neighborhood gray feature. Firstly, the pixels on ice cream bar surface are clustered according to information of position and gray level, after which gaining some regions with similar gray level, then the candidate contamination regions are extracted using fuzzy rule. At last, the absolute neighborhood gray feature is defined after feature analysis towards contamination texture, through which the contamination regions are recognized accurately.

2 Image Acquisition, Feature Analysis and Preprocess

2.1 Image Acquisition

Fig.1 is the image of ice cream bar acquired by the home-made image acquisition device, the size is 1280 * 512. The bar located in the bottom is the target of this paper, and the above is used for other defects which are not the contents of this paper. The imaging sensor used in this paper is area-array cameras of XIMEA, and the illuminating apparatus is strip-shaped white light source of OPT. The cameras

and illuminating apparatus are installed above the band carrier, and the camera would be triggered to grab image when the ice cream bar passes. Fig.2 is the image acquisition device.

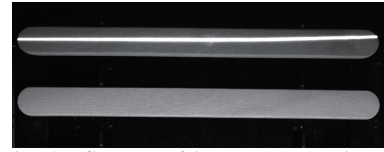


Fig. 1 Sample of ice cream bar image

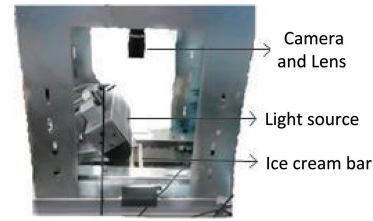
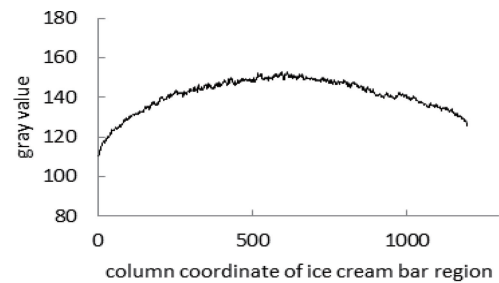


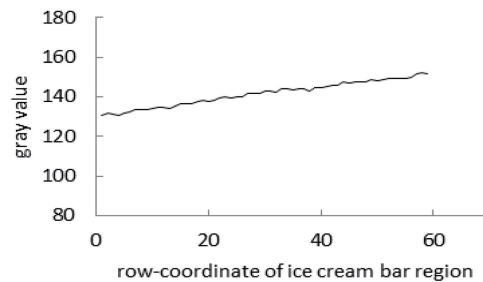
Fig. 2 Image acquisition device

2.2 Feature Analysis of the Defect

As the ice cream bar moves on the band carrier, it could not be ensured that the bar is always located on the center of light band, which makes the nonuniform of illumination on ice cream bar. It could be seen through the horizontal and vertical projection curve in Fig.3. The middle region is lighter than the two terminals.



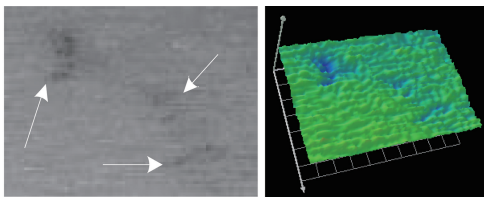
(a) Vertical projection curve



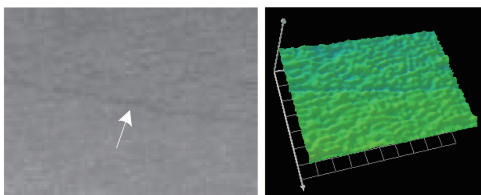
(b) Horizontal projection curve

Fig. 3 Horizontal and vertical projection curve of target ice cream bar

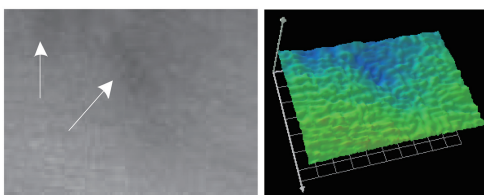
Fig.4 (a) is the image of contamination region on ice cream bar and its three-dimensional grayscale distribution. Actually, contamination is the dark areas on the ice cream bar infected with blot in the process of mechanical transmission. The contamination is with the uncertain shape, various size and different color depth, which makes the detection harder. As seen meanwhile, the contamination is hollow and represents flocculent with no obvious edge. As the three-dimensional grayscale distribution image shown, the gray value of contamination region is lower than its neighbourhood, which could be the sally port for contamination defect detection. While there are some wooden texture and dark spot on the bar, and their gray value is also lower than their neighbourhood, shown as the white arrow in Fig.4 (b), (c). So how to distinguish contamination from them is the crucial problem.



(a) Contamination and its three-dimensional grayscale distribution



(b) Wooden texture and its three-dimensional grayscale distribution



(c) Dark spot and its three-dimensional grayscale distribution

Fig. 4 Dark region on ice cream bar and their three-dimensional grayscale distribution

2.3 Preprocess of Icecream Bar Image

The preprocessing is for extracting the above target ice cream bar as the ROI, which is used for later algorithm treatment. In literature^[16], aiming at the location, the rough location is carried out firstly, then segment is carried out using OTSU, which achieves superior performance. So this method is used in this paper, and the effect is shown as Fig.5, with the outline of target ice cream bar region marked in red line.



Fig. 5 Effect of preprocessing

3 Extraction of Nominated Contamination Region Based on Adjacent Gray Level Clustering and Fuzzy Rule

The contamination region could be extracted from the perspective of gray level according to the above analysis. The gray level of pixels are concentrated relatively both in contamination regions and background regions (the word 'background' refers to the surface of ice cream bar where it is clean, and it is consistent in the follow paragraphs), and there are some gray differences between contamination and background. So, it is a feasible to pick out contamination region from subdomains which are obtained via dividing the ice cream bar surface into sub-regions according to the gray level.

3.1 Definition and Application of Adjacent Gray Level Clustering

Clustering is one of the most important application of computer vision, and it is mainly used to classify the target objects in image^[17-18]. The purpose of clustering in this paper is dividing the region of contamination and background into different regions. A multi-classification arithmetic of 'neighbouring-grayscale' clustering is proposed, which is based on the gray level of pixels being concentrated in contaminated regions. The word 'neighbouring' in

neighbouring-grayscale' refers to the adjacent spatial position, and the word 'grayscale' is the gist of pixels clustering. Two principles are set to guide the operation of the clustering arithmetic concretely.

1. It exists $d_{ist} \leq d_t$, and d_{ist} is the minimum distance between two pixel sets which are waiting to be classified. The value of d_t is 1 which signifies the spatial position of the two pixel sets adjacent in 8-neighborhood. The specific definition of d_{ist} is shown as formula (1).

2. The gray relationship between two pixel sets which waited to be classified must be satisfied with the condition: $G_{rel} \leq g_t$. The definition of G_{rel} is shown as formula (2), and g_t is the gray threshold which is set to 2.

$$d_{ist} = \min_{\substack{(a1,b1) \in \Gamma \\ (a2,b2) \in X}} \Psi[(a1,b1), (a2,b2)] \quad (1)$$

$$G_{rel} = abs(\{g(a1,b1) - \theta(a1,b1)\}) \quad (2)$$

In formula (1), Γ and X represents two pixel sets which are waiting to be classified respectively, $(a1, b1)$ represents the coordinate position in the image of Γ , $(a2, b2)$ represents the coordinate position in the image of X , and $\Psi[(a1, b1), (a2, b2)]$ represents the Euclidean distance between $(a1, b1)$ and $(a2, b2)$. In formula (2), $g(a1, b1)$ represents the gray value of $(a1, b1)$, and $\theta(a1, b1)$ represents the gray average of n pixels which belongs to set X and is adjacent with the 8 neighborhoods of $(a1, b1)$. If $n=0$, the value of $\theta(a1, b1)$ is set to $g(a1, b1) + g_t + 1$.

The detailed procedures of the neighbouring-grayscale clustering arithmetic is shown as following under the above principles.

1. Select the top left corner pixel $(0, 0)$ as the initial position of object image region.

2. Compute the grayval relationship feature G_{rel} of the point $(0+u, 0+v)$ and $(0, 0)$. If the condition is $G_{rel} \leq g_t$, the point $(0+u, 0+v)$ and $(0, 0)$ will be clustered as one set and the set is marked as A00, and the step 3 is executed with the initial position $(0+u, 0+v)$ which is marked as $(i0, j0)$. If the condition is $G_{rel} > g_t$, the point $(0, 0)$ will be clus-

tered as a sole set (marked as A00) and stored into the set Ω to indicate that this point has been calculated, then the step 4 is executed. The range of u and v in the above is from -1 to 1. And $(0+u, 0+v)$ is the adjacent pixel of $(0, 0)$ in 8-neighborhood.

3. Compute the grayval relationship feature G_{rel} of the point $(i0+u, j0+v)$ and $(i0, j0)$. If the condition is $G_{rel} \leq g_t$, they will be clustered as one set solely (marked as $Ai0j0$), and is put into Ω meanwhile. Finishing the clustering operation when $G_{rel} > g_t$ and then step 4 is executed. And G_{rel} as mentioned above is the gray relationship between $(i0, j0)$ and $(i0+u, j0+v)$ which is the adjacent pixel of $(i0, j0)$ in 8-neighborhood.

4. The initial point (x, y) is selected renewedly, with $x = \min(i')$, $y = \min(j')$, $(i', j') \in \Phi$. The definition of Φ is shown in formula (3). The point (x, y) is marked as $(i0, j0)$ and then Step 4 is executed when Φ is not empty. Otherwise, the arithmetic is finished.

$$\Phi = A_{ROI} \odot \Omega \quad (3)$$

In formula (3), A_{ROI} is the point set belonging to the ice cream bar object region, and \odot represents the operation of remainder taking.

3.2 Extraction of Nominated Contamination Region Using Fuzzy Rule

It is hard to describe the contamination texture because of its fickle shape, inconsistent size and different depth, but these ambiguous concepts could be described adequately via fuzzy theory^[19-20]. At present, fuzzy theory is applied in reality more and more frequently. The relevant theory of fuzzy set is adopted to describe the contamination texture in this paper, and the contamination and non-contamination texture are classified preliminarily via the relevant theory of fuzzy set.

The object ice cream bar region has been divided into some sub-regions via the arithmetic in section 3.1. The method to extract the regions of contamination from these sub-regions is the subject matter of this part. Fuzzy rules and some available characteris-

tics of the sub-regions are used to select contamination regions roughly.

Rule 1:

The region is a suspected contamination, if the value G_m of region is biggish.

The definition of G_m is mentioned in the rule above, shown as formula (4). In formula (4), p represents the sequence number of the regions partitioned as figure 6. $Mean(p)$ represents the gray average of p th region in figure 6, (p, q) represents the sequence number of the grandson region q in the p th region, and $Mean(p, q)$ represents the gray average of q th grandson region. The grandson region mentioned hereinbefore is divided by the arithmetic of neighbouring-grayscale clustering in section 3.1.

$$G_m = Mean(p) - Mean(p, q) \quad (4)$$

The ice cream bar surface region is divided into a few pieces to avoid the influence of uneven illumination, as shown in figure 6. The phenomenon of nonuniform illumination generally in vertical and horizontal direction can be known from section 2, but the partial gray fluctuation is lesser. So the entire ice cream bar surface region is divided into $m * n$ subdomains. The specific method to divid the entire ice cream bar surface region is minimum enclosing rectangle. Then, R is segmentated into m ($m=5$) parts in width and n ($n=3$) parts in length. A griding that type is $3 * 5$ is obtained via the operation mentioned above. The compartment is marked as $W_p, p=1, 2, \dots, m * n$. Then S_p is the desired subdomain, $S_p = W_p \cap A_{ROI}$.

The regions which are obtained via the clustering algorithm in the scope of S_p are the subdomains of S_p and the grandson regions of the ROI. Some regions obtained via the clustering algorithm in 3.1 are splitted into multiple smaller regions by the gridding (marked as black full line), shown as figure 7. In Fig.7, r is splitted into 5 parts as the number marked when the ubiety of r and gridding are the same to Fig.7, then each part becomes one of the subdomains of the corresponding sub-boxes and the grandson regions of the ROI. The splitted part of r will partici-

pate in the operation of formula (4) as the form of grandson region. And r is the gray area in Fig.7 which is the sketch map of a region obtained via the clustering algorithm hereinbefore.



Fig. 6 Division of subregions

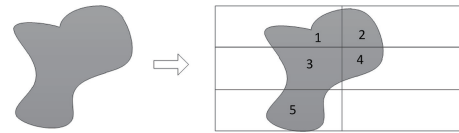


Fig. 7 Division of grandson regions

The ‘biggish’ is a fuzzy conception in Rule 1. A method of statistics combined with inference is used to establish the function $u_{large}(x)$, which is the membership degree of ‘biggish’. A set number of typical contamination defect samples are selected to be observed and counted. The value G_m of contamination is greater than 5 by statistics of the samples, then the value of $u_{large}(x)$ is set to 1 when $G_m > 5$. The value of G_m is set to 0 because the grandson region should not be contaminated when the gray of grandson region is equal to the relevant subdomain. The middle part between 0 and 5 is expressed with linearity. And $u_{small}(x)$ is the membership degree function of ‘lesser’ symmetry in $u_{large}(x)$. The curve of $u_{small}(x)$ and $u_{large}(x)$ is shown as Fig.8. Fig. 9 is the processing effect of Fig.6 via Rule 1, which is based on the principle of maximal degree of membership.

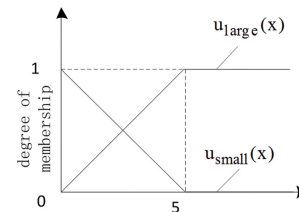


Fig. 8 Membership functions of ‘Biggish’ and ‘lesser’



Fig. 9 Nominated contamination regions extracted by rule 1

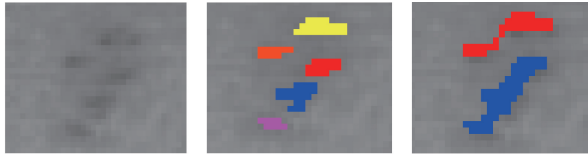
Rule 2:

The region is a suspected contamination, if the area Ar of the region is biggish.

When these smaller regions are satisfied with Rule 1, it is reasonable to merge the regions which belong to one piece of contamination but are clustered to many smaller regions via the operation of section 3.1. So the operation of merging adjacent domains is done before the executing of Rule 2. The method of merge is morphological closing operation as shown in formula (5) and the effect is shown as Fig.10.

$$\Psi(a) = C_{ir} \otimes (C_{ir} \oplus a) \quad (5)$$

In formula (5), letter a represents the processed region, C_{ir} represents the circular structure element which radius is 3, and \oplus and \otimes represent the dilation and erosion of morphology respectively.



(a) Certain contamination region (b) Processing effect of Rule 1 (c) Effect after merging

Fig. 10 Effect after merging contamination regions

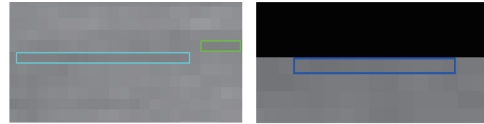
The region with smaller area could be dislodged via its area value because the contamination is not existing in the form of a sole pixel or few pixels through observing.

Rule 3:

The region is not contaminated, if w - is lesser AND the orientation of O_{ri} and the long axis orientation λ of ice cream bar ROI are ‘approximate’.

In Rule 3, w - represents the mean width of the object region and O_{ri} represents the displacement distance towards the object region. The orientation of long axis and minor axis is obtained via the method of document^[10], the orientation of long axis is O_{ri} , and the average pixel quantity in minor axis of the object region is w -. The long axis orientation λ of ROI is obtained via the method of document^[10] similarly.

The purpose of Rule 3 is dislodging the regions of wood fiber and marginal noise (shown in Fig.11) which is retained after the operation of Rule 1 reasoning for its lower gray. However, the orientations of wood fiber and marginal noise are always along the long axis of the ice cream bar. Wood fiber and marginal noise are linear in shape and narrow in width relatively. The displacement distance and width are randomly opposite. So the wood fiber and marginal noise could be dislodged via this rule.



(a) Region of wood fiber (b) Region of edge noise

Fig. 11 Regions of wood fiber and edge noise in nominated regions after treatment by Rule 1

The ‘biggish’ in Rule 2 and the ‘lesser’, ‘approximate’ in Rule 3 are all fuzzy parameters, and function of fuzzy membership is established. As the Ar of contaminations is always greater than 8 and the Ar of noise regions is always less than 5 through observing the images in image database. So the value of $u_{large-a}(x)$ is set to 1 when $Ar > 8$, the value of $u_{large-a}(x)$ is set to 0 when $Ar < 5$, and the distribution between 5 and 8 is linear. And $u_{small-a}(x)$ which is the subordinating degree function of ‘lesser’ is symmetrical with $u_{large-a}(x)$. The $u_{small-a}(x)$ and $u_{large-a}(x)$ are shown in Fig.12 (a). As the w - of contaminations is always greater than 4 and the Ar of noise regions is less than 3 through observing the images in image database. So the value of $u_{small-w}(x)$ is set to 0 when $w - > 4$, the value of $u_{small-w}(x)$ is set to 1 when $Ar < 3$, and the distribution between 3 and 4 is linear. The $u_{large-w}(x)$ which is the subordinating degree function of ‘biggish’ is symmetrical with $u_{small-w}(x)$. And $u_{small-w}(x)$ and $u_{large-w}(x)$ are shown in Fig.12 (b). The subordinating degree function of ‘approximate’ (marked as $u_{near}(x)$) and ‘removed’ (marked as $u_{far}(x)$) is shown as Fig.12 (c), the abscissa shows the differential seat angle between the displacement distance towards object re-

gion and the long axis direction of ROI.

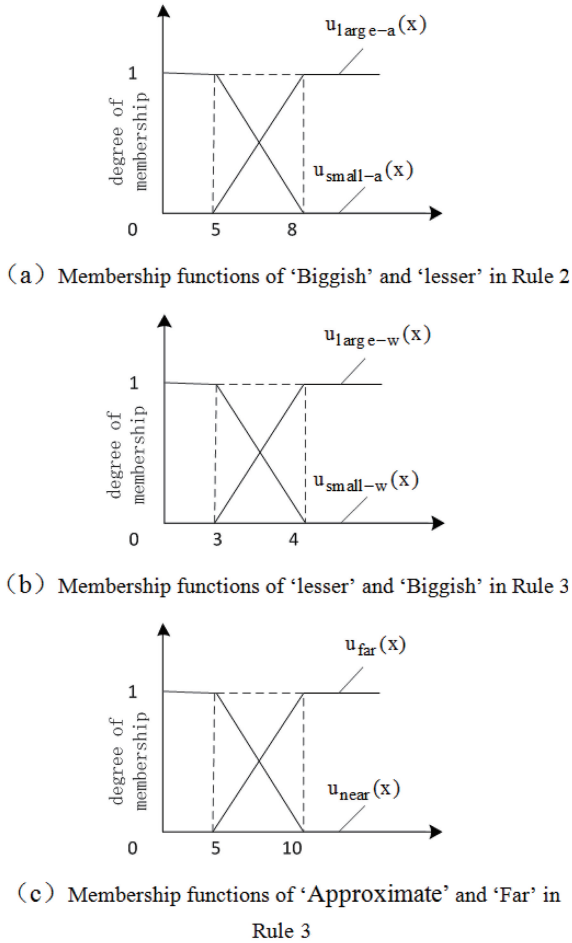


Fig. 12 Membership function of rule 2 and rule 3

4 Accurate Extraction of Contamination Regions Based on Absolute Neighborhood

The nominated contamination regions obtained from section 3 not only have the true contamination regions but also contain the wooden texture and dim spot. Therefore, an absolute neighbourhood method is presented to recognize the true contamination regions. The basic process is as follows.

4.1 Formulating a dictionary for pixel location

Depositing all the pixel locations of the nominated contamination regions obtained from section 3 into a dictionary which will be used later. The location dictionary is composed of a matrix and the capacity

of the matrix is $2 * (n+1)$ as shown in Fig.13. The regions obtained from section 3 are traversed point by point and processed according to Formula (6). The target pixel column coordinates (marked as x') are stored in row 0 of the matrix, the row coordinates (marked as y') are stored in row 1 of the matrix. The scope of x' is from 0 to $H-1$. The scope of y' is from 0 to $W-1$. The 'H' and 'W' mentioned in the above represent the height and width respectively. Then the max length of the dictionary is $n = (H * W) - 1$.

$$\begin{cases} g(x', y') = 1, \text{add to Dictionary} \\ g(x', y') = 0, \text{no-operation} \end{cases} \quad (6)$$

a00	a01	a02	a03	a0n
a10	a11	a12	a13	a1n

Fig. 13 Dictionary about pixel location

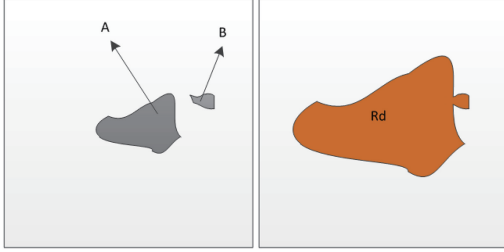
4.2 Acquiring the absolute neighbourhood

The nominated regions H obtained from section 3 are constrained-dilated using the defined circular flat structure elements ξ that radius is h . It can be represented as $\delta_\xi(H)$, shown as formula (7). The process and effect are shown as Fig. 14. Taking an example of region A in Fig.14(a), the region R_d is acquired through hitting region A using the structure element ξ , which could be regarded as a point set of position. And the pixels location in region R_d is likely to be the absolute neighbourhood location of A. Then each pixel location is checked according to the dictionary (marked as D), which is obtained in step 1 for confirming whether the pixel location belongs to R_d . The pixels belonging to D would be wiped off. The members of set R_d are also wiped off if they are not located in the ROI and the value of h is set to 8 in this paper.

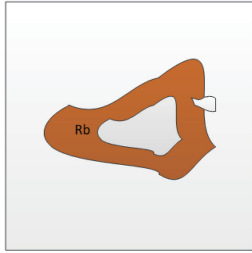
$$\delta_R(H) = \{ (i, j) \mid [\xi_x \cap H \neq \emptyset] \text{AND} [(i, j) \notin D] \text{AND} [(i, j) \subset \Omega] \} \quad (7)$$

In formula 7, x represents the circle center of the structural element and ξ_x represents a set of points which is composed of the pixels that covered with ξ

when the centre of structure element ξ is located at x ($(i, j) \in \xi_x$), ξ_x represents the set of pixel location which is in the range of region ROI.



(a) Nominated contamination regions (b) Dilation effect of A



(c) Constrained-dilation effect of A

Fig. 14 Effect of dilation and constrained-dilation

4.3 Extracting contamination region accurately

The connected region H is verdicted to confirm whether it is contaminated via formula (8).

$$H = \begin{cases} \text{ture}, e - F > t \\ \text{false}, e - F \leq t \end{cases} \quad (8)$$

In formula (8), 'ture' signifiys H is contamination, and 'false' signifiys H is not contamination. t is the threshold value, which is determined through the experiment. The definition of F is shown as formula (9).

$$F = \frac{1}{d(N/2) - 1} \sum_{i=1}^{d(N/2)} \gamma(i) \quad (9)$$

In formula (9), γ is a array which is composed of the pixel value in region A in descending order. $\gamma(i)$ denotes the value of the member of i in γ , N denotes the pixel number of region A, and $d(*)$ denotes the operation of the biggish integer. The physical significance of F is the gray average of the half pixels with low grey value in nominated region. The reason of defining F as formula (9) is that the interior of contamination is flocculent. The darker

pixels are real contamination. Then it is more reasonable to calculate according to formula (9) instead of the method of average value like literature^[16].

5 Experiment Design and Result Analysis

The image database called SUT-D is established with 156 contamination ice cream bar images and 147 normal ice cream bar images, which is used to verify the algorithm. There are 189 blocks of contamination texture that are calibrated by manual work in the 156 contamination ice cream bar images. The computer that is used for algorithm testing has 2G RAM, Intel Core i3 processor, 2.10 GHz dominant frequency and Windows 7 32-bit professional edition Service Pack 1 operating system. The algorithm platform for the experiment is Visual Studio C++ 2010.

5.1 Detection Process of Contamination Defect

The specific detection process of contamination on the ice cream bar is as follows.

1. Read in the ice cream bar image.

2. Get the region of interesting (ROI) on ice cream bar image.

3. The ROI is clustered via the neighbouring-grayscale algorithm, and the nominated contamination regions are extracted via fuzzy rule which includes contamination, wood grain and macula. Maximum membership degree is used to judge the corresponding region, combining with the fuzzy value which is acquired from three defined principles.

4. The absolute neighbourhood arithmetic is used to recognize the contamination region precisely. The outline gray value of contamination regions is set to 255 to facilitate observation and demonstration.

5.2 Experiment Result Analysis

The accuracy of contamination detection CDR_d , the normal ice cream bar correct recognition rate CDR_c and the total accuracy CDR_f are defined for assessing the proposed algorithm in this paper.

$$CDR_d = \frac{C_d}{A_d} \times 100\% \quad (10)$$

$$CDR_c = \frac{C_c}{A_c} \times 100\% \quad (11)$$

In formula (10), C_d means the quantity of contamination regions which are detected accurately, and A_d means the quantity of total contaminat regions. In formula (11), C_c means the quantity of normal ice cream bars which are judged as zero defect and A_c means the quantity of total normal ice cream bars.

$$CDR_f = \frac{C_f}{A_f} \times 100\% \quad (12)$$

In formula (12), C_d=C_d+C_c, A_f=A_d+A_c.

5.2.1 Determination of Threshold t

Fig.15 is the curve of CDR_f distribution in different value of t, which is the threshold of the gray feature of absolute neighbourhood. The figure shows that the CDR_f reaches to 0.9732, which is the maximum value in the curve when t equals to 15. So the value of t is confirmed to 15 finally.

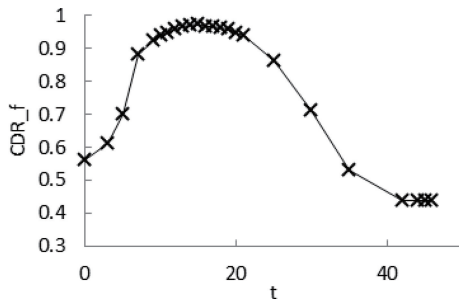


Fig. 15 distribution curve of CDR_f

5.2.2 Experiment Effect and Contrast Analysis

Fig. 16 is the detection result when t = 15. It shows that the shallow contamination can be extracted successfully and the mottled background texture can be excluded successfully in the meantime.

There are 156 contamination images and 147 normal ice cream bar images in the image database. By using the proposed algorithm, the examination of these images is to test the contamination texture recognition performance and the robustness for background texture.

Firstly, the images of ice cream bar with contamination are tested via the proposed algorithm. 185

blocks of contamination regions are detected successfully. The CDR_d is 97.88 percent. Then the 147 normal ice cream bars are tested via the proposed algorithm also. 5 ice cream bars are detected mistakenly. The CDR_c is 96.60 percent. The detailed testing result is shown in Table1. The CDR_f can be calculated via formula (12) and the result is 97.32 percent.

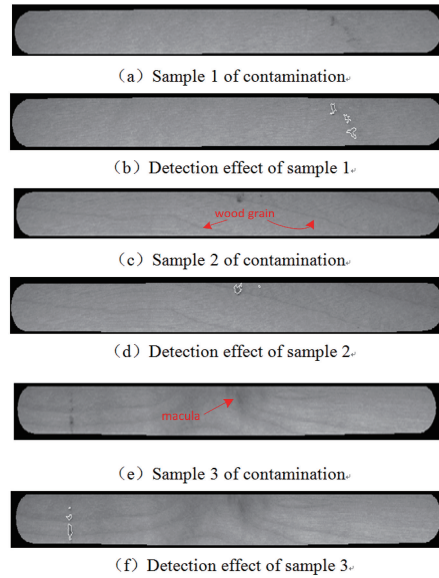


Fig. 16 Samples of contamination and detection effect

Table 1 Testing results

Sample database	Quantity of samples	Quantity of defect	Quantity of correct detection	Rate of correct detection
Contamination image	150	189	185(piece)	97.88%
Normal image	144	0	142(piece)	96.60%

Some other contamination detection methods are compared with the proposed algorithm in this paper, and the results are shown in Table 2.

Table 2 Experiment results contrast

Method	CDR_f(%)
Histogram ^[15]	91.96
Local threshold segment ^[14]	93.15
Constraint rules ^[16]	94.64
This paper method	97.32

It is shown in Table 2 that the value of CDR_f algorithm is higher than other methods, which displays the prominent advantage and proves the effectiveness.

The cases of missing detection and false detection are observed and analyzed. The case of missing detection is shown as Fig.17. Fig.17(a) is the original image of ice cream bar with contamination, Fig. 17(b) is the image of detection effect. As seen, most of the contamination region is detected successfully except the region which is marked by the red arrow. The reason of missing detection is that the gray value is very close to the background which causes the gray feature of absolute neighbourhood is less than the given threshold value.

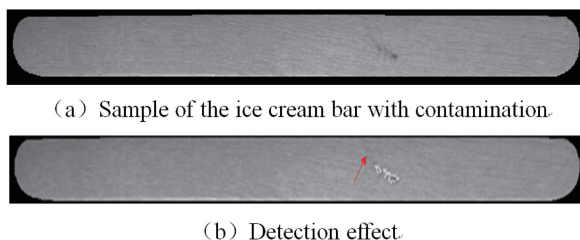


Fig. 17 Sample of contamination missing detection

Fig.18 is the ice cream bar detected mistakenly which is normal actually. The reason of false detection is that the gray value of wood texture is comparatively small which causes the gray feature of absolute neighbourhood greater than the given threshold value.

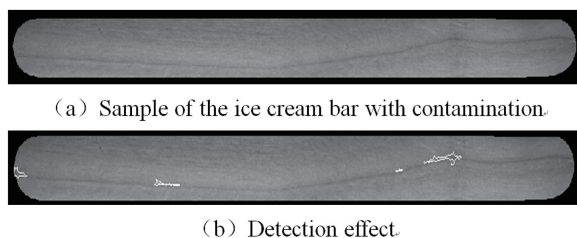


Fig. 18 Sample of contamination false detection

6 Conclusion

Contamination detection is the important content of ice cream bar surface quality detection system.

But the fickle shape, inconsistent size, different depth, flocculent interior and fuzzy edge make the detection of contamination rather difficult, which resulting in poor arithmetic effect. Aiming at this problem, this paper puts forward a detection method. Firstly, the object regions are roughly select sketchily via fuzzy rule. Then the contamination is recognized precisely via the defined gray feature of absolute neighbourhood. In this paper, arithmetic principle is expounded detailedly, image database is established for experiment, and setting method of typical parameters is introduced. Finally, the method proposed in this paper is tested in the image database and the implementation result is analyzed. The results show that the CDR_f could reach to 97.32% and improved 2.68% at least comparing with other methods. The experimental results proves the advantage and the practical application value.

References

- [1] WANG Yuchun. Introduction of ice cream bar production technology [J], Journal of Forestry Engineering, 1993, (3):22.
- [2] CHENG Lijia. Design of Ice Cream Bar Quality Detection System Based on Online Visual Inspection [D]. Shenyang University of Technology, 2016.
- [3] WU Zhiren, WANG Dehua. The length detection device of the ice cream bar and Ice cream bar automatic inspection machine with this device; CN 203605910 U [P]. 2014-05-21.
- [4] WU Zhiren, HUO Fulin. The Buckling test device on Ice cream bar automatic inspection machine; CN2498580 [P]. 2002-07-03.
- [5] XIE Bingjiang, FANG Maokui. Ice cream bar bar automatic sorting machine; CN2612246 [P]. 2004.
- [6] BOGUE R W. Machine Vision Theory, Algorithms, Practicalities [J]. Assembly Automation, 2005, 25 (3):58.
- [7] DAHJYE L, ROBERT S, JAMES A, et al. Development of a machine vision system for automatic date grading using digital reflective near-infrared imaging [J]. Journal of Food Engineering, 2008, 86(3):388-398.
- [8] Favret C, Sieracki J M. Machine vision automated species identification scaled towards production levels [J].

- Systematic Entomology, 2016, 41(1):133-143.
- [9] YUAN Wweiqi ,LI Shaoli,LI Dejian . Wood surface defects recognition based on sub-region zoom Gaussian fitting [J]. Chinese Journal of Scientific Instrument, 2016, 37(4):879-886.
- [10] YUAN Wweiqi , LI Dejian , LI Shaoli. Online method based on machine vision for measuring contour quality of ice cream stick [J]. Application research of computer, 2016, 33(10), 3185-3190
- [11] SHHNORBANUN S, HUDA S N, HASLINA A, et al. A computational biological network for wood defect classification [J]. Lecture Notes in Engineering and Computer Science, 2010, 2186(1):559-563.
- [12] ZHANG Y ZH, XU CH, LI CH, et al. Wood defect detection method with PCA feature fusion and compressed sensing [J]. Journal of Forestry Research, 2015, 26(3):745-751.
- [13] GU I Y, ANDERESSON H, VICEN R. Wood defect classification based on image analysis and support vector machines [J]. Wood Science and Technology, 2010, 44(4):693-704.
- [14] CHEN Dan. Research on Defects Detection of Surface in Ice Cream Bar [D]. Shenyang university of technology, 2016
- [15] SONG Xiaoyan. Research on Image Analysis Method of Wood Surface Gray Defects Recognition [D]. Inner Mongolia University of Technology, 2015.
- [16] LI Shaoli, YUAN Weiqi, LI Dejian. Detection of contamination defects on the surface of the ice cream bar based on the Union-Find Sets and constraint sets [J/OL]. Application research of computers. 2018 (2017-07-21). <http://kns.cnki.net/kcms/detail/51.1196.TP.20170721.1354.080.html> .
- [17] Shakeri M, Dezfoulian M H, Khotanlou H, et al. Image contrast enhancement using fuzzy clustering with adaptive cluster parameter and sub-histogram equalization [J]. Digital Signal Processing, 2017, 62:224-237.
- [18] Bahadure N B, Ray A K, Thethi H P. Performance analysis of image segmentation using watershed algorithm, fuzzy C-means of clustering algorithm and Simulink design [C]// International Conference on Computing for Sustainable Global Development. IEEE, 2016.
- [19] Yang L, Chao F, Shen Q. Generalised Adaptive Fuzzy Rule Interpolation [J]. IEEE Transactions on Fuzzy Systems, 2017, PP(99):1-1.
- [20] Sánchez L, Couso I. A framework for learning fuzzy rule-based models with epistemic set-valued data and generalized loss functions [J]. International Journal of Approximate Reasoning, 2017.

Authors' Biographies



Li Shaoli, (Corresponding author) received B.Sc. from Shenyang University of Technology in 2013. Now she is a doctoral candidate in Computer Vision Group, Shenyang University of Technology. Her research interests include machine vision and biometric identification.

E-mail: 707816215@qq.com



Yuan Weiqi, received B. Sc. degree from Hunan University in 1982, received M. Sc and Ph. D degrees both from Northeastern University in 1988 and 1997, respectively. Now he is a professor and doctoral supervisor in Shenyang University of Technology. His research interests include machine vision and biometric identification.

E-mail: yuan60@126.com